Fracture behaviour of grain refined A356 cast aluminium alloy: tensile and Charpy impact specimens

D. Casari, A. Fortini, M. Merlin
Department of Engineering, University of Ferrara, Ferrara (Italy)
daniele.casari@unife.it, annalisa.fortini@unife.it, mattia.merlin@unife.it

SUMMARY. The excellent combination of high strength/weight ratio, high impact toughness, very good castability, low thermal expansion coefficient and corrosion resistance make Al-Si cast alloys suitable for the production of components like rims, engine and gear parts. Even though it is well-known that mechanical properties are closely related to secondary dendrite arm spacing (SDAS), the influence of grain size has to be considered as well. A fine and equiaxial grain structure is generally obtained through specific products, called grain refiners, which are added to the melt alloy in form of cans, bars, tabs, waffles, ingots and granulated fluxes. In this study three commercial Ti-B based grain refiners were added to the A356 (Al-Si-Mg) aluminium alloy. A number of 20 castings was obtained through permanent mould casting, n°5 for each experimental condition, named Reference (not refined), GR1, GR2 and GR3. Tensile and Charpy impact specimens were drawn by means of machining, T6 heat-treated and then tested. The influence of the grain refiners was assessed according to the experimental data of tensile and impact tests. Experimental results were compared to OM and SEM fracture observations, pointing out the effect of the different grain refiners on fracture mechanism. Although both impact and tensile specimens showed a mixed transgranular-intergranular fracture mode, it was found that impact samples were deeply influenced by the refiner added, while this effect was less pronounced for the tensile ones. Fractographic observations also revealed the role of Fe based intermetallic compounds in terms of fracture behaviour.

KEYWORDS. Grain refinement; Tensile and impact tests; Intermetallic compounds.

INTRODUCTION

Al-Si cast alloys are widely used alloys in the automotive field because of their good castability, their high strength/weight ratio, their corrosion and wear resistance and their excellent recycling behaviour. In particular, the A356 (Al-Si-Mg) is one of the most used: in this alloy, Mg is added as a key alloying element in order to induce age hardening by means of fine precipitation of Mg_2Si particles. The microstructure of as-cast A356 alloy is made up of coarse primary α-Al dendrites and acicular-shaped eutectic Si particles, which determine low mechanical properties and limit its industrial applications. It is well-known that mechanical properties and fracture mechanisms are strongly affected by the secondary dendrite arm spacing (SDAS), the morphology and distribution of eutectic Si particles and secondary phases [1-3]. Ductility, fatigue and tensile strength are limited by the dendritic structure and non-uniform distribution of acicular Si particles [4]. The Fe content in these cast alloys is generally considerated negative because of his tendency to form harmful intermetallic compounds whose morphology is dependent upon cooling conditions and alloying elements content [5,6]. In presence of Si, Fe is deleterious because of the precipitation of β-Al_5FeSi platelets and the subsequent decrease of mechanical properties, such as tensile strength, toughness and ductility. When, in addition to Si, is also present Mg, the π-$Al_8FeMg_3Si_6$ intermetallic compound can be formed.

For the industrial propose, grain refinement and modification, performed by the addition of Ti and Sr respectively, are employed to improve the mechanical properties of the castings, by refining the micro-constituents (α-Al and eutectic Si particles) [7]. Unmodified acicular Si particles act as internal stress risers and provide easy path for fracture; the dendrite arm spacing and the cell size also affect the low fracture toughness of these alloys. Hence, the improvement of the mechanical properties is closely related to type, shape and size of secondary phases. The modification of eutectic Al-Si-Mg alloys has considerable effect on the microstructure, as it determines a reduction of size and aspect ratio of eutectic Si particles. Moreover, the addition of Al-Ti and Al-Ti-B master alloys to aluminium converts large elongated α-Al grains into fine and equiaxed ones: a fine and randomly oriented equiaxed grain structure improves mechanical and fatigue properties of castings [7]. For this reason, grain refinement has become a standard treatment practice in aluminium foundries worldwide [8]. The introduction of inoculating particles into melts has proved to be the most effective way to achieve small uniformly distributed equiaxed grains, which leads to high toughness, high yield strength, excellent formability and improved machinability [9-11]. The most widely used grain refiners are based on Al-Ti, Al-B, Al-Ti-B or Al-Ti-C systems and many theories have been proposed to explain the mechanism of grain refinement [12-14]. It is accepted that both the addition of nucleant particles (TiB_2, TiC, Al_3Ti) and segregating elements are necessary for a good outcome of the treatment. The potential of Al-B master alloy in the grain refinement of aluminium foundry alloys has been recently investigated by Chen et al. [15]: they reported that the AlSi7Mg alloy exhibits the highest improvement in tensile properties compared to Al-Zn, Al-Cu, Al-Mg alloys. Tensile strength and ductility were greatly improved, confirming the Al-B master alloy potential as a powerful grain refiner for Al-Si foundry alloys with high Si contents. Li et al. [16] have found that an improved grain refinement performance of the A356 alloy can be achieved through the addition of 0.2 wt.% Al-3Ti-1B-0.2C master alloy: they found that the best combination of both strength and ductility is due to the finer grains resulting from the refinement by means of the Al-3Ti-1B-0.2C master alloy compared to the Al–5Ti–1B one. Many authors have investigated the effect of different chemical and metallurgical aspects on the impact properties of Al-Si-Mg alloys. Murali et al. [17] assessed the influence of Mg and Fe on impact toughness of AlSiMg0.3 alloys, finding that an increase of both elements, in a specific range, leads to a decrease of the total absorbed energy. More recently, Alexopoulos et al. [18] have assessed the effect of artificial aging on the impact mechanical behaviour of A357 cast aluminium alloy; in particular, they have found that on the one hand the maximum load increases as the aging time raises, but on the other hand this implies a decrease of the total absorbed energy. Merlin et al. [19], by means of tests performed on A356-T6 sub-size Charpy impact specimens, have proved that casting defects nearby the V-notch have a strong detrimental effect on impact toughness and they become dominant compared to microstructural features. Only a recent study has considered the effect of the grain refinement on the impact properties of A356 aluminium alloy: Casari et al. [20] have found that Ti-B based grain refiners cause a decrease in terms of maximum load and total absorbed energy.
The aim of the present work is to show the effects of three commercial Ti-B based grain refiners (in form of can, tab, and granulated flux) on fracture behaviour of A356 foundry aluminium alloy. Tensile and Charpy impact tests were performed to compare mechanical properties to fracture mechanisms, which were evaluated by means of optical and scanning electron microscopy analyses. Fractographic observations were carried out to investigate the fracture mechanisms and the role of the intermetallic compounds involved in the crack process.

EXPERIMENTAL PROCEDURE

A commercial A356 aluminium alloy, whose chemical composition is shown in Tab. 1, was melted in an electric-induction furnace and held at 750 ± 5 °C. For the eutectic Si modification, several bars of Al-10 wt% Sr master alloy were added to reach the target Sr level of 200 ppm; the melt was then degassed for 10 min by means of argon inert gas. At the same time, the melt was stirred and grain refined through the addition of three commercial Ti-B based grain refiners in form of can, tab and granulated flux, which were named GR1, GR2 and GR3 respectively. The grain refiners' quantities were fixed in one can, one tab and 300 g of powder, in order to compare the effects of the two one-piece grain refiners to a proportional amount of granular flux. However, it should be pointed out that, due to the different chemical composition of the grain refiners, an equal weight does not correspond to an equal grain refinement effect.
A number of 20 castings, n°5 for each experimental condition (Reference, GR1, GR2 and GR3) were realised by pouring the alloys into a steel mould; one tensile specimen and one Charpy impact specimen were drawn by means of machining from each casting (Fig. 1).

Si	Fe	Cu	Mn	Mg	Cr	Zn	Ni	Ti	B
6.9000	0.1240	0.0075	0.0071	0.3390	<0.0100	0.0128	<0.0030	0.136	<0.005
Sn	**Ag**	**Zr**	**Ca**	**Pb**	**Sr**	**Na**	**Li**	**P**	**Al**
<0.0009	<0.0004	0.0010	<0.0010	<0.0012	0.0094	0.0017	0.0008	<0.0010	bal.

Table 1: Chemical composition (wt. %) of the A356.0 aluminium alloy.

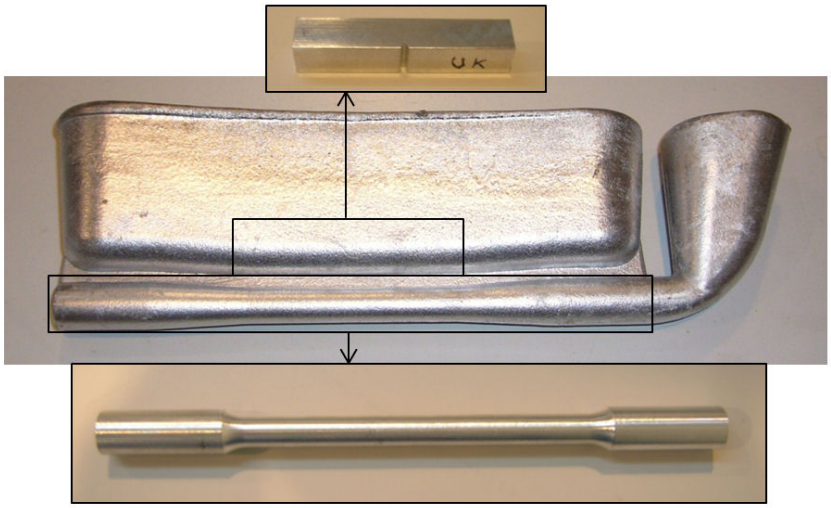

Figure 1: Casting design used in the experiments [20]. The *black boxes* indicate the regions where tensile and Charpy impact specimens were drawn.

The tensile specimens, machined according to the ASTM E8-04 specification (40 mm gauge length and 8.5 mm diameter), and the Charpy specimens, machined according to the UNI EN ISO 148-1 specification (10x10x55 mm) were T6 heat-treated. Hence, they were heated up to 520 °C for 4 h, quenched in a solution of water and glycol at 25 °C and subsequently aged at 160 °C for 6 h and cooled in calm air. The tensile tests were carried out at room temperature, using an MTS 810 Material Testing System. Test parameters were set by means of the MPT Software: crosshead speed was fixed at 0.02 mm/s and the applied load was restricted to 40 kN. Stress-strain curves were obtained by attaching a knife-edge extensometer to the specimens' gauge length and the tensile properties were determined from the digital files. The impact tests were performed on a CEAST instrumented Charpy pendulum, according to the ASTM E-23 specification. The total impact energy (*Wt*), calculated as the integral of load-displacement curve, was determined by means of a dedicated software connected to a data acquisition system. After tensile and impact tests, all fracture surfaces were observed and examined by means of optical microscopy (OM) and scanning electron microscopy (SEM). For the metallographic examination, a section perpendicular to the fracture surface was cut from one of the halves of each sample and subsequently embedded in phenolic resin for standard grinding and polishing procedures. The samples were etched with a HF (0.5%) aqueous solution to better identify the intermetallic compounds and the optical observations were carried out by means of a LEICA MEF4M microscope. The remaining fracture surfaces of the tensile and Charpy specimens were analysed by a ZEISS EVO 40 electron microscope and by energy dispersive X-ray spectroscopy, to evaluate the fracture mode and the nature of the intermetallic compounds.

RESULTS AND DISCUSSION

The effect of grain refiners on the tensile and impact properties of A356 alloy was studied by testing refined (GR1, GR2 and GR3) and not refined (Reference) samples. The average values of the experimental tests, as well as their standard deviations, are shown in Tab. 2.

It is observed that, apart from a small increase in the yield strengths, the tensile properties are not influenced by the addition of grain refiners to the melt when compared to the Reference. Conversely, the detrimental effect of grain refinement on total absorbed energy (*Wt*) is remarkable. The average value of GR3 total absorbed energy has the lowest deviation from the Reference one, indicating that the powder seems to have a less deleterious effect than GR1 and GR2.

It is also possible to observe that the addition of grain refiners leads to a general decrease in the standard deviations of tensile and impact data. This reduction is linked to the better microstructural homogeneity achieved by the addition of grain refiners to the melt, in terms of decrease in grain size and intermetallics distribution in the interdendritic regions.

	$Rp_{0,2}$ [MPa]	**UTS** [MPa]	**A%**	**Wt** [J]
Reference	245.2 ± 4.6	319.4 ± 4.0	11.3 ± 1.4	4.8 ± 1.1
GR1 (Can)	251.5 ± 3.4	320.9 ± 5.0	11.0 ± 1.0	3.3 ± 1.1
GR2 (Tab)	250.6 ± 1.7	320.4 ± 2.6	11.5 ± 1.0	3.4 ± 0.5
GR3 (Granular flux)	249.2 ± 1.8	320.6 ± 1.7	11.3 ± 1.3	4.0 ± 0.9

Table 2: Experimental results of tensile and impact tests.

As can be seen in Fig. 2 (a-d), the microstructure of both the Reference and grain refined alloys consists of a primary α-Al solid phase and an Al-Si eutectic mixture. The addition of the grain refiners to the molten alloy causes a massive heterogeneous nucleation during cooling. Therefore, the α-Al primary phase morphology changes from fully columnar (dendritic) to equiaxed. The morphology of the eutectic Si particles is fibrous, as a result of the addition of Sr to the melt. Intermetallic Fe-based compounds, such as β-Al_5FeSi platelets, are also found. Optical microscopy observations reveal that β-Al_5FeSi platelets are larger for the impact specimens than for the tensile ones. In their complementary work, Casari et al. found that the average maximum length of β-Al_5FeSi platelets ranges from 19 (Reference) to 35 μm (GR1) for the impact specimens [20]. Conversely, these intermetallic compounds are more difficult to observe in the tensile samples.

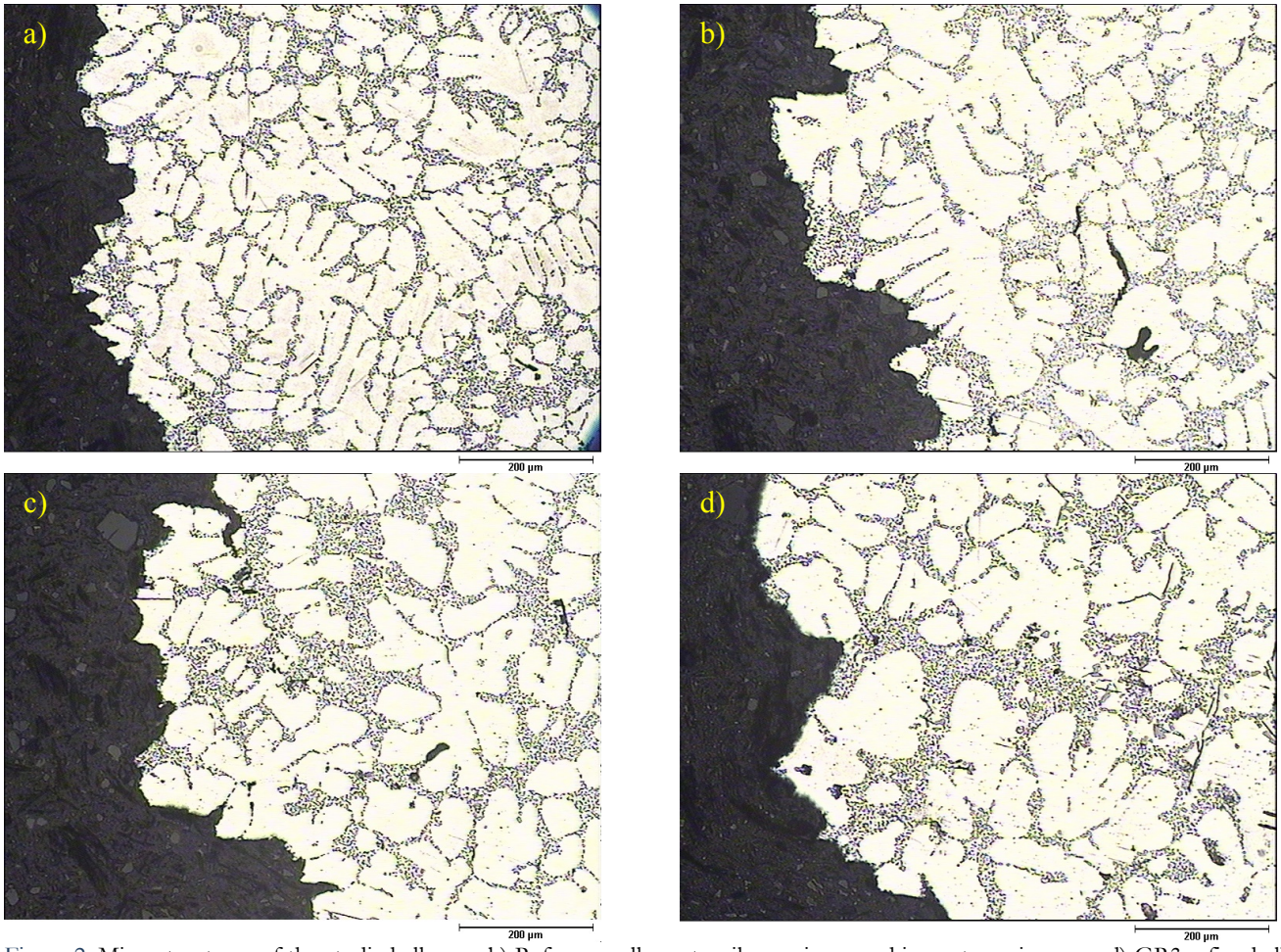

Figure 2: Microstructures of the studied alloys: a-b) Reference alloy – tensile specimen and impact specimens; c-d) GR3 refined alloy – tensile and impact specimens.

This is due to the more severe cooling rate of the tensile specimens with respect to the impact ones, which were obtained from the feeders. It is well-known that the size and morphology of the Fe-rich phases are not only dependent on alloy composition, but also on the cooling rate [21]. Increasing the solidification rate is a well-established method to control the amount and size of the β-platelets.
As already stated, none of the grain refiners affected the tensile properties. The high cooling rate related to the metal mould mostly influenced the solidification and the mechanical properties of the tensile specimens by decreasing both the SDAS and the size and amount of β-Al_5FeSi intermetallic compounds. This basically led to the same high performances for all the studied alloys. Conversely, the influence of grain refiners on the impact specimens was significant because of the lower cooling rate of the metal in the feeder. As a consequence, two opposite situations took place, depending on the effectiveness of the grain refiner: on the one hand, when GR1 and GR2 were added, grain refinement positive effect, related to the decrease in grain size, was exceeded by the negative one related to the increase in SDAS [20]; on the other hand the addition of GR3 to the molten alloy led to the development of a larger grain boundary array, which positively influenced the fracture behaviour as discussed below, and to a better distribution of intermetallic compounds.
Both the Reference and the refined alloys show a mixed transgranular-intergranular fracture mode at optical microscopy examinations [1,3], with no substantial differences between the tensile and the impact specimens. As can be seen in Fig. 3, the fracture profile follows a preferential path through the eutectic phase, sometimes dividing a secondary dendrite arm from the following one. Although a small plastic deformation can occur, in particular just in the last stages of the test, the more ductile α-Al primary phase is generally not involved in the fracture process. Fracture growth involves mainly the cracking of Si particles and acicular β-Al_5FeSi intermetallics due to the formation of internal stresses in the particles by plastic deformation (Fig. 4). Once the particle cracks, a microvoid is formed and tends to grow. This particle cracking process continues until a critical volume fraction of cracked particles is reached. The consequent rapid linking process among microcracks eventually leads to the alloy failure.

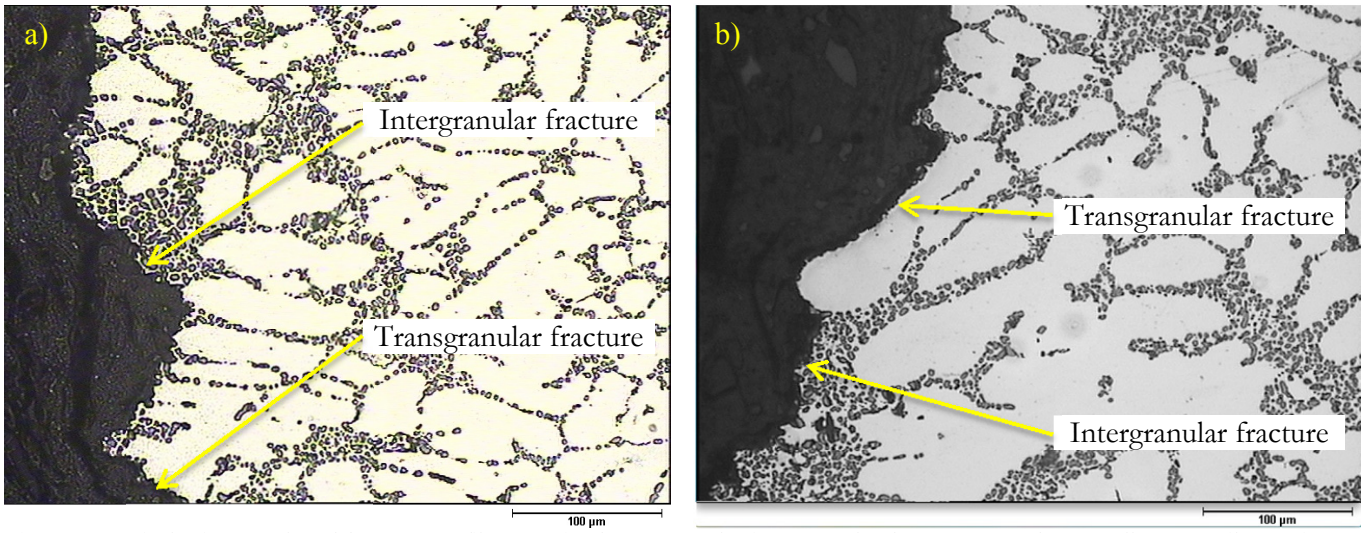

Figure 3: Optical micrographs of fracture profiles: a) Mixed transgranular-intergranular fracture on Reference alloy – tensile specimen; b) Mixed transgranular-intergranular fracture on GR3 refined alloy – tensile specimen.

It has been proved that this mixed fracture behaviour is mostly related to SDAS size [3,20,22]. In fact, when SDAS is large, eutectic Si particles precipitate not only at the grain boundaries but also between the secondary arms. Eutectic Si particles, Fe-based intermetallic compounds and their interfaces with the aluminium matrix are more fragile than the α-Al primary phase itself. When fracture starts, eutectic and β-Al_5FeSi platelets between the secondary dendrite arms provides an easier path for its propagation with respect to the ones spread through the more irregular grain boundary zone, which would require a larger energy amount [1,21,23]. Moreover, as previously observed, β-Al_5FeSi intermetallics were only found along the fracture profiles of the impact specimens due to their lower cooling rate (Fig. 4).
The SEM analysis of the fracture surfaces confirms the mixed transgranular–intergranular fracture mode. However, as can be seen in Fig. 5 (a-b), the intergranular fracture mode is prevalent for the tensile specimens in all the studied alloys, whereas the impact specimens of the grain refined alloys show a considerable amount of transgranular fracture (i.e. lower

amount of total absorbed energy). The fracture surface is mainly ductile; the edges of the deformed and fractured micronecks in both transgranular and intergranular eutectic regions can be easily distinguished. This is due to the specific damage process of the A356 alloy, which starts with the cracking of Si and β-Al_5FeSi particles caused by high local plastic strain (Fig. 6). The presence of secondary phases was revealed on the fracture surfaces of both tensile and Charpy impact samples in the interdendritic paths of fracture or emerging from the microvoids. The analysis with the EDS microprobe indicates the nature of the precipitates as brittle β-Al_5FeSi platelets (Fig. 7).

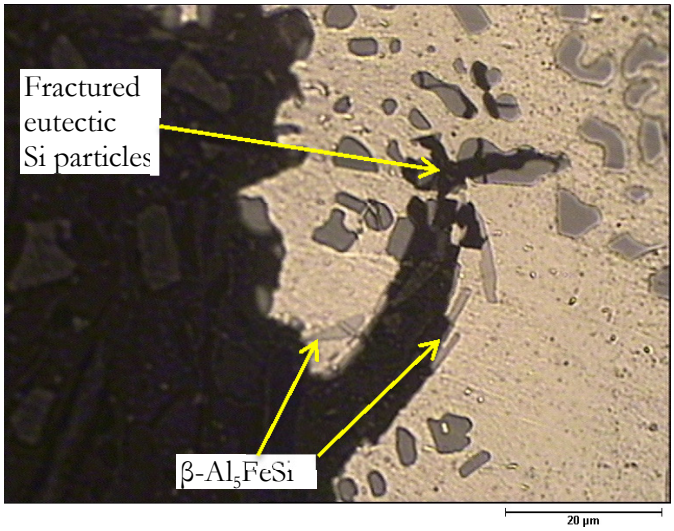

Figure 4: Fractured acicular β-Al_5FeSi intermetallics and eutectic Si particles along and near the fracture profile of a Charpy impact specimen.

It has been proved that this mixed fracture behaviour is mostly related to SDAS size [3,20,22]. In fact, when SDAS is large, eutectic Si particles precipitate not only at the grain boundaries but also between the secondary arms. Eutectic Si particles, Fe-based intermetallic compounds and their interfaces with the aluminium matrix are more fragile than the α-Al primary phase itself. When fracture starts, eutectic and β-Al_5FeSi platelets between the secondary dendrite arms provides an easier path for its propagation with respect to the ones spread through the more irregular grain boundary zone, which would require a larger energy amount [1, 21, 23]. Moreover, as previously observed, β-Al_5FeSi intermetallics were only found along the fracture profiles of the impact specimens due to their lower cooling rate (Fig. 4).
The SEM analysis of the fracture surfaces confirms the mixed transgranular–intergranular fracture mode. However, as can be seen in Fig. 5 (a-b), the intergranular fracture mode is prevalent for the tensile specimens in all the studied alloys, whereas the impact specimens of the grain refined alloys show a considerable amount of transgranular fracture (i.e. lower amount of total absorbed energy). The fracture surface is mainly ductile; the edges of the deformed and fractured micronecks in both transgranular and intergranular eutectic regions can be easily distinguished. This is due to the specific damage process of the A356 alloy, which starts with the cracking of Si and β-Al_5FeSi particles caused by high local plastic strain (Fig. 6). The presence of secondary phases was revealed on the fracture surfaces of both tensile and Charpy impact samples in the interdendritic paths of fracture or emerging from the microvoids. The analysis with the EDS microprobe indicates the nature of the precipitates as brittle β-Al_5FeSi platelets (Fig. 7).
These observations justify the previous assumptions about both the tensile and impact data. As far as tensile samples are concerned, the fracture behaviour is the same because of the predominance of the cooling rate (i.e. small SDAS and low amount of Fe-rich intermetallics), thus leading to the same mechanical properties for the Reference and the grain refined alloys. Regarding impact specimens, cooling rate becomes less important, so that fracture mode and total absorbed energy average values change because of the opposite effects linked to the effectiveness of grain refiners. Therefore, while GR1 and GR2 alloys have the highest detrimental effect with respect to Reference, GR3 addition leads to a fracture propagation which is not mainly transgranular, but continuously shifts from transgranular to intergranular, thus absorbing a larger amount of energy.

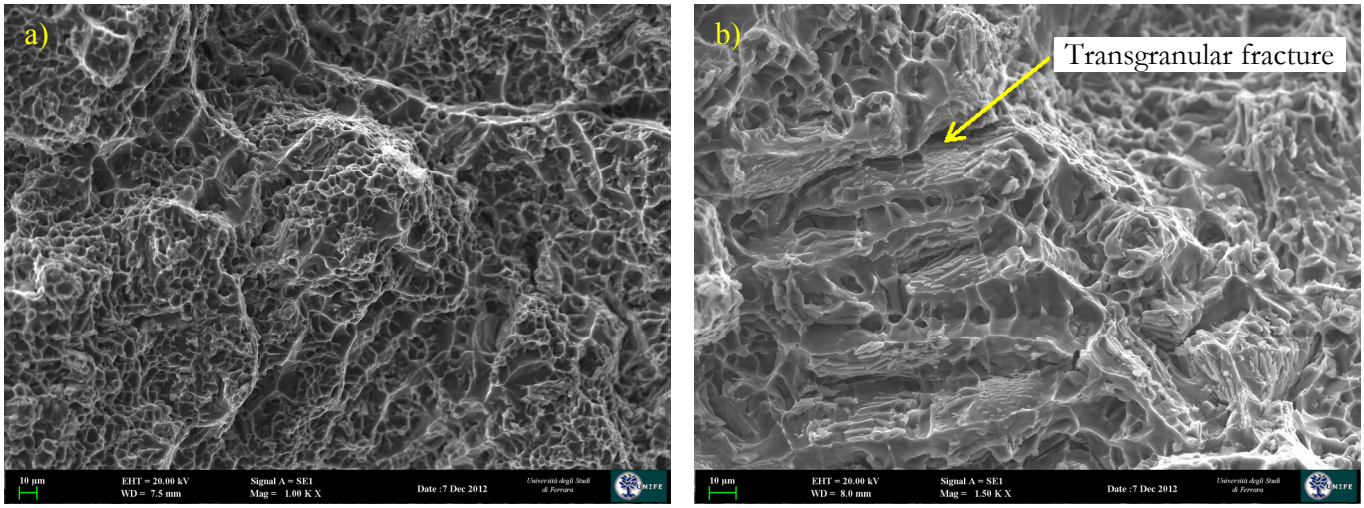

Figure 5: SEM fractographs: a) Mostly intergranular fracture mode on tensile specimen (high magnification); b) Mixed transgranular-intergranular fracture mode on Charpy impact specimen (high magnification).

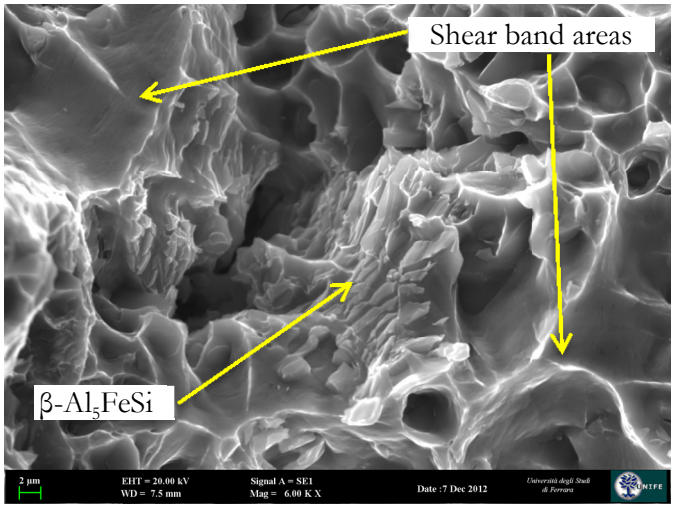

Figure 6: Cracking of β-Al_5FeSi particles caused by high local plastic strain at the tip of the microvoid.

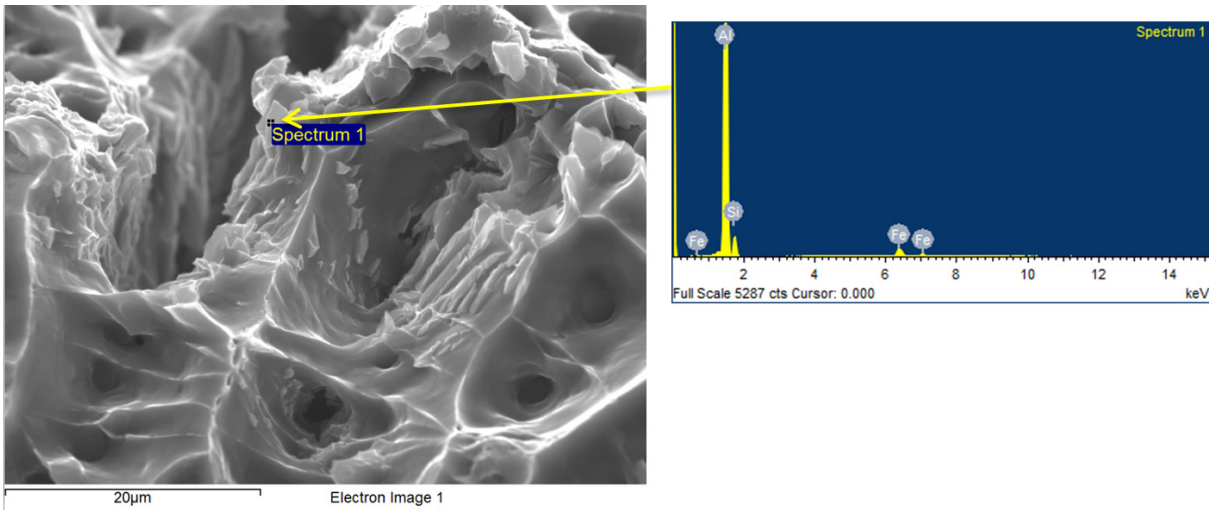

Figure 7: EDS microprobe analysis of a β-Al_5FeSi intermetallic observed on the fracture surface of a tensile specimen.

CONCLUSIONS

Three commercial Ti-B based grain refiners were added to A356 cast aluminium alloy. The effect of grain refiners on the fracture behaviour of tensile and Charpy impact specimens was investigated by means of optical and scanning electron microscopy observations. The concluding remarks are as follows:

1. Apart from a small increase in the yield strengths, the tensile properties are not influenced by the addition of grain refiners to the melt when compared to the Reference, whereas the detrimental effect of grain refinement on total absorbed energy (*Wt*) is significant.
2. Both the Reference and the refined alloys exhibit a mixed transgranular-intergranular fracture mode at optical microscope examination, with no substantial differences between the tensile and the impact specimens. However, SEM observations show that the intergranular fracture mode is prevalent for the tensile specimens in all the studied alloys, whereas the impact specimens of the grain refined alloys show a considerable amount of transgranular fracture.
3. None of the grain refiners affects the tensile properties. Cooling rate controls the solidification in terms of SDAS and distribution of the Fe-based intermetallic compounds and, as a consequence, the fracture behaviour of the tensile specimens, leading to the same mechanical properties for all the studied alloys.
4. The contribution of cooling rate to impact properties is negligible, so that fracture mode and total absorbed energy average values change because of the opposite effects linked to the effectiveness of grain refiners. While GR1 and GR2 alloys have the highest detrimental effect with respect to Reference, GR3 addition leads to a fracture propagation which is not mainly transgranular, but continuously shifts from transgranular to intergranular, thus absorbing a larger amount of energy.

REFERENCES

[1] Q. G. Wang, Metallurgical and materials transactions A, 34A (2003) 2887.
[2] R. E. Spear, G.R. Gardner, AFS Transactions, 71 (1963) 209.
[3] C. H. Cácares, C. J. Davidson, J. R. Griffiths, Materials Science and Engineering A, 197 (1995) 171.
[4] Y. Birol, Journal of Alloys and Compounds, 486 (2000) 219.
[5] M. Merlin, La Metallurgia Italiana, 3 (2010), 37.
[6] B. Suárez-Pena, J. Assensio-Lozano, Scripta Materialia, 54 (2006) 1543.
[7] S. Haro-Rodríguez et al., Materials and Design, 32 (2011) 1865.
[8] Y. Birol, Journal of Alloys and Compounds, 420 (2006) 71.
[9] Y. Birol, Journal of Alloys and Compounds, 513 (2012) 150.
[10] Y.F. Han et al. , Materials Science and Engineering A, 405 (2005) 306.
[11] M. A. Easton, D.H. Stjohn, Acta Materialia, 49 (2001) 1867.
[12] B. S. Murty et al. , International Materials Reviews, 47 (2002) 3.
[13] D. G. McCartney, International Materials Reviews, 34 (1989) 247.
[14] K. T. Kashyap, T. Chandrashekar, Bulletin of Materials Science, 24 (2001) 345.
[15] Z. Chen et al., Materials Science and Engineering A, 553 (2012) 32.
[16] P. Li et al. , Materials and Design, 47 (2013) 522.
[17] S. Murali et al. , Materials Science and Engineering A, 151 (1992) 1.
[18] N.D. Alexopoulos, A. Stylianos, Materials Science and Engineering A, 528 (2011) 6303.
[19] M. Merlin et al., Journal of Materials Processing Technology, 209 (2009), 1060.
[20] D. Casari et al., Journal of Material Science, 48 (2013) 4365.
[21] O. Vorren et al., AFS Transactions, 92 (1984) 459.
[22] C. H. Cáceres, J.R. Griffiths, Acta Materialia, 44 (1996) 25.
[23] Z. Ma et al., AFS Transactions, 101 (2003) 255.